

Numerical Study of Quantum Hall Bilayers at Total Filling $\nu_T = 1$: A New Phase at Intermediate Layer Distances

Zheng Zhu,¹ Liang Fu,¹ and D. N. Sheng²

¹*Department of Physics, Massachusetts Institute of Technology, Cambridge, MA, 02139, USA*

²*Department of Physics and Astronomy, California State University, Northridge, CA, 91330, USA*

We study the phase diagram of quantum Hall bilayer systems with total filling $\nu_T = 1/2 + 1/2$ of the lowest Landau level as a function of layer distances d . Based on numerical exact diagonalization calculations, we obtain three distinct phases, including an exciton superfluid phase with spontaneous interlayer coherence at small d , a composite Fermi liquid at large d , and an intermediate phase for $1.1 < d/l_B < 1.8$ (l_B is the magnetic length). The transition from the exciton superfluid to the intermediate phase is identified by (i) a dramatic change in the Berry curvature of the ground state under twisted boundary conditions on the two layers; (ii) an energy level crossing of the first excited state. The transition from the intermediate phase to the composite Fermi liquid is identified by the vanishing of the exciton superfluid stiffness. Furthermore, from our finite-size study, the energy cost of transferring one electron between the layers shows an even-odd effect and possibly extrapolates to a finite value in the thermodynamic limit. Our identification of an intermediate phase and its distinctive features sheds new light on the theoretical understanding of the quantum Hall bilayer system at total filling $\nu_T = 1$.

PACS numbers: 73.21.Ac, 73.43.-f, 73.21.-b

Introduction.—Multi-component electron systems subject to a perpendicular magnetic field open an intriguing realm for strongly correlated physics due to the degrees of freedom among different components. In particular, the multi-layer quantum Hall systems demonstrate tremendously rich physics when tuning the interlayer interaction by changing layer distance d . One of the prominent examples is the bilayer systems^{1–4} at a total filling $\nu_T = 1$ ($\nu = 1/2$ in each layer) with negligible tunneling. Experimentally, the bilayer systems can be realized in single wide quantum wells, double quantum wells or bilayer graphenes^{5–9}.

Theoretically, the quantum states in small and large d limits have been well understood. When the layer distance goes to zero, the strong interlayer coulomb interaction drives the electron system into a pseudospin (layer) ferromagnetic long range order (FMLRO) state with the spontaneous interlayer phase coherence and interlayer superfluidity^{10–14}. The FMLRO can also be described as an exciton condensation state as an electron in an orbit of one layer is always bound to a hole in another layer forming an exciton pair. When the layer distance is small but finite, the difference between the interlayer and intralayer Coulomb interactions breaks the pseudospin $SU(2)$ invariance down to $U(1)$, leading to an easy-plane pseudospin ferromagnet. This excitonic superfluid state can be described by Haldane’s “111 state” wavefunction^{15,16}. In the limit of infinite layer separation, the bilayer system reduces to two decoupled composite Fermi liquids (CFL)^{17–21}.

Several theoretical scenarios^{22–34} have been proposed for understanding the transition between the exciton superfluid and CFL at intermediate layer distances. Due to its non-perturbative nature, controlled analytical method for this problem is so far lacking, and numerical techniques have been playing an important role. Some numerical studies report a single phase transition, or a crossover, between the small and large distance regimes^{35,36}. This is also consistent with exact diagonalization (ED) studies including weak disorder effects³⁷. On the other hand, an intermediate phase is found in ED and variational studies^{39–42}, where the p -wave paired

composite fermions state^{40,41} is proposed. It remains unsettled whether there exists a distinct phase at intermediate distances.

On the experimental side, transport measurements indicate a transition between incompressible FQH state and compressible liquid as a function of the layer distance^{43–46}. At smaller layer distance, the total Hall conductance is quantized to e^2/h . A strong enhancement in the zero-bias interlayer tunneling conductance⁴⁷ and the vanishing of the Hall counterflow resistance^{46,48} provide evidence for interlayer coherence⁴. Above a critical distance $d \approx 1.6 \sim 2$ (in units of magnetic length l_B) which depends on the quantum well thickness, a compressible liquid state is found^{4,43–50}. However, the nature of the state at the intermediate distance has not been settled after numerous experimental investigation⁴.

Motivated by this unsolved issue, in this work we carry out an extensive numerical study of $\nu = 1/2 + 1/2$ bilayer system, with a focus on the intermediate layer distance regime. We perform ED on torus, which is a suitable geometry for studying competing compressible and incompressible states^{51,52}. Taking advantage of all commuting magnetic translational symmetries⁵¹, we reach the largest system size up to 20 electrons in ED, which allows for a robust finite-size scaling analysis for such systems. Our numerical phase diagram is summarized in Fig. 1. We identify signatures of two phase transitions between the “111 state” and the CFL at critical distances $d_{c1} \approx 1.1$ and $d_{c2} \approx 1.8$, respectively. For layer distance $d < d_{c1}$, we establish the excitonic superfluid state by the existence of Goldstone mode, vanishing of single pseudospin excitation gap and finite exciton superfluid stiffness. Furthermore, the interlayer pseudospin Berry curvature shows strong fluctuation, leading to non-quantized drag Hall conductance which is consistent with the gapless feature of the “111 state”. On the other hand, for the intermediate layer distance $d_{c1} < d < d_{c2}$, we find the gapped single pseudospin excitation which is combined with a finite exciton superfluid stiffness. The drag Hall conductance is quantized to zero with no singularity in the pseudospin Berry curvature in this regime while the total Hall conductance remains exactly quantized to

e^2/h . The quantum phase transition between the exciton condensed “111 state” and intermediate phase is identified by a dramatic change in the Berry curvature of the ground state under twisted boundary conditions on the two layers, and the level crossing with a change of the nature of the low-lying excitations at $d = d_{c1}$. The fact of level crossing near d_{c1} is consistent with previous studies^{36,39,42}. The second transition between the intermediate phase and the CFL is characterized by the vanishing of the exciton superfluid stiffness. We compare the low energy spectrum near d_{c2} with the decoupled CFL state at $d = \infty$, and discuss the related finite-size effect in the supplementary materials.

Model and Method.— We consider bilayer electron systems subject to a magnetic field perpendicular to the two dimensional (2D) planes. We use torus geometry with the length vectors \mathbf{L}_x and \mathbf{L}_y , and an aspect angle θ between them. Here, $L_x = L_y = L$ and $\theta = \pi/2$ for most of calculations. The magnetic length $l_B \equiv \sqrt{\hbar c/eB} \equiv 1$ is set to be the unit of the length and N_ϕ represents the number of magnetic flux quanta determined by $|L_x L_y \sin \theta| = 2\pi N_\phi$. In the presence of strong magnetic field, the Coulomb interaction, projected onto the lowest Landau level, is written as

$$V = \frac{1}{2\pi N_\phi} \sum_{i < j, \alpha, \beta} \sum_{\mathbf{q}, \mathbf{q} \neq 0} V_{\alpha\beta}(\mathbf{q}) e^{-q^2/2} e^{i\mathbf{q} \cdot (\mathbf{R}_{\alpha,i} - \mathbf{R}_{\beta,j})}. \quad (1)$$

Here, $\alpha(\beta) = 1, 2$ are indices of two layers (which are the two components of a pseudospin 1/2), $V_{\alpha,\alpha}(\mathbf{q}) = 2\pi e^2/(\varepsilon q)$ and $V_{12}(\mathbf{q}) = V_{21}(\mathbf{q}) = 2\pi e^2/(\varepsilon q) \cdot e^{-qd}$ are the Fourier transformations of the intralayer and interlayer Coulomb interactions, respectively. d is the distance between two layers and $\mathbf{R}_{\alpha,i}$ is the guiding center coordinate of the i th electron in layer α . In the present work, we consider the physical systems with two identical 2D layers (with zero width) and without electron interlayer tunneling while spins of electrons are fully polarized due to strongly magnetic field.

We use ED algorithm to study the energy spectrum and state information on torus. In order to study the physics of the pseudospin sector, we generalize the periodical boundary condition to twist boundary condition $T^\alpha(\mathbf{L}_\lambda) |\Phi\rangle = e^{i\theta_\lambda^\alpha} |\Phi\rangle$ ($\lambda = x, y$), where $T^\alpha(\mathbf{L}_\lambda)$ is the magnetic translational operator and $0 \leq \theta_\lambda^\alpha \leq 2\pi$ is the twisted boundary phase in λ direction in the layer α . By a unitary transformation, one can get the the periodic wave function Ψ on torus with

$$|\Psi\rangle = \exp \left[-i \sum_{\alpha} \sum_i \left((\theta_x^\alpha/L_x) x_i^\alpha + (\theta_y^\alpha/L_y) y_i^\alpha \right) \right] |\Phi\rangle. \quad (2)$$

Then the Berry curvature is defined by $F(\theta_x^\alpha, \theta_y^\beta) = i(\langle \partial\Psi/\partial\theta_x^\alpha | \partial\Psi/\partial\theta_y^\beta \rangle - \langle \partial\Psi/\partial\theta_y^\beta | \partial\Psi/\partial\theta_x^\alpha \rangle)$. The integral over the boundary phase unit cell leads to the topological Chern number matrix $C_{\alpha,\beta} = 1/2\pi \int d\theta_x^\alpha d\theta_y^\beta F(\theta_x^\alpha, \theta_y^\beta)$, which contains topological information for the bilayer quantum Hall state^{37,53–55}. Numerically, applying common and opposite boundary phases on two layers, one can obtain the Hall conductances in the layer symmetric and antisymmetric channel, denoted by $C^c(e^2/h)$ and $C^s(e^2/h)$, respec-

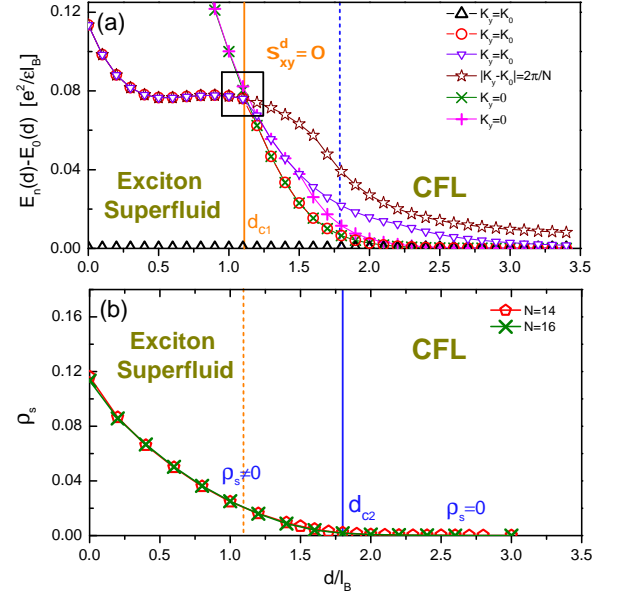


Fig. 1: (Color online) The phase diagram of $\nu = 1/2 + 1/2$ quantum Hall bilayers with varying layer distance d/l_B . We identify three phases: exciton superfluid phase, the intermediate phase and composite Fermi liquid (CFL) phase. (a) The transition from exciton superfluid to intermediate phase near $d_{c1} \approx 1.1$ is identified by the drag Hall conductance σ_{xy}^d and the energy level crossing for $N = 16$ electron system. Here, the ground state is in the momentum sector $K_0 = \pi$. (b) The transition from intermediate phase to CFL phase near $d_{c2} \approx 1.8$ is identified by the exciton superfluid stiffness ρ_s [see Eq. 3].

tively. The drag Hall conductance, defined by $\sigma_{xy}^d = (C^c - C^s)(e^2/2h) = (C_{1,2} + C_{2,1})(e^2/h)$, can be obtained directly by calculating $C_{1,2}$ (or $C_{2,1}$), corresponding to twisting boundary phases along x direction in one layer and along y direction in another layer. One can also obtain the exciton superfluid stiffness when applying twisted boundary phases³⁷.

Energy Spectrum and Pseudospin Excitation Gap.— At zero or smaller layer separation d , the pseudospin FMLRO indicates the gapless pseudospin excitations, i.e., the Goldstone mode. In Fig. 2 (a), we show the lowest energies in each momentum sector for different layer distances d . For smaller layer separations $d \lesssim 1.1$, indeed we find the low energy excitation has the form of linear dispersing Goldstone mode for small momenta. One can also measure the pseudospin excitation gap directly, which represents the energy cost of moving one electron from one layer to another layer and is defined as $\Delta_{ps}(d) \equiv E_0(N_\uparrow, N_\downarrow, d) - E_0(N/2, N/2, d) + d \cdot S_z^2/N_\phi$. Here, $N_\uparrow = N/2 + \Delta N$ and $N_\downarrow = N/2 - \Delta N$ denote the number of electrons in two layers for $S_z = \Delta N = 1, 2, \dots$ excitation. The energy shift $d \cdot S_z^2/N_\phi$ is the charge energy induced by the imbalance of electron number in two layers with total pseudospin S_z ⁵⁶. As shown in Fig. 2 (b), the $\Delta_{sp}(d)$ for $S_z = 1$ drops with the number of electron N , and the finite size scaling of the gap $\Delta_{ps}(d)$ for $S_z = 1$ goes to zero in the thermodynamic limit for $d \lesssim 1.1$, consistent with the gap-

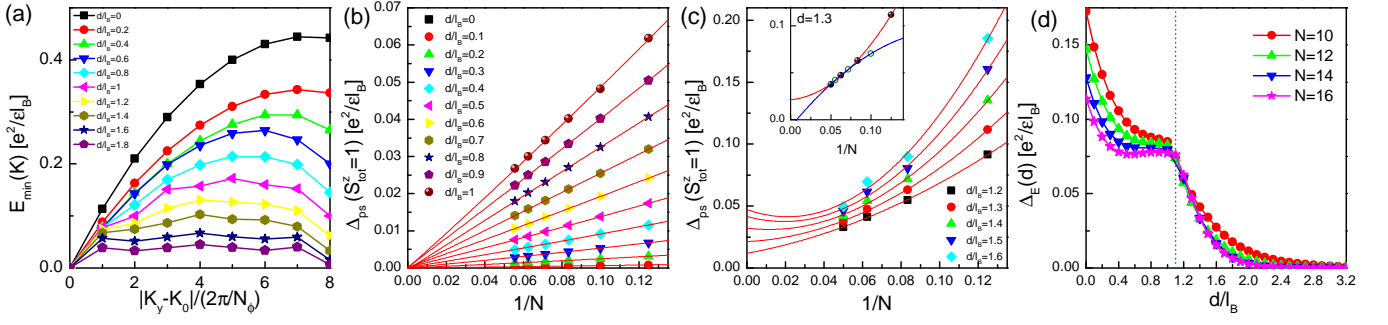


Fig. 2: (Color online) (a) The energy dispersion curves of lowest-energy excitations at each momentum sector. Here, the ground state is in the momentum sector $K_0 = \pi$. (b) and (c) show finite size scaling of the single pseudospin excitation gap Δ_{ps} by using parabola function for layer distance $d/l_B < 1.1$ (b) and $d/l_B > 1.1$ (c). The inset of (c) indicates the even-odd effect in the intermediate phase up to $N = 20$. (d) The energy spectrum gap $\Delta_E \equiv E_1(d) - E_0(d)$ as a function of d/l_B . The cusp near $d/l_B \approx 1.1$ indicates the level crossing for the excited states.

less pseudospin excitations. Here, the ground state is in the momentum sector $K_0 = \pi$.

On the other hand, for layer distance $d \gtrsim 1.1$, the low energy linear dispersion spectrum (the Goldstone mode) moves up in energy [see Fig. 2 (a)] with new lower energy excitations appearing at other momenta sector for $d \gtrsim 1.1$ as shown in Fig. 1. For the layer distance $d \approx 1.1$, the energy spectrum shows the level crossing of the first excited states between the $K_y = \pi$ (or $K_y = 0$) and $|K_y - K_0| = 2\pi/N$ sectors (see more complete spectrum in Fig. 1). Although the ground state still locates in $K_y = K_0$ sector at $d \approx 1.1$, the level crossing for the first excited state indicates the change of the low-lying energy spectrum for the bilayer systems.

For $d \gtrsim 1.1$, the $S_z = 1$ pseudospin excitation displays even-odd effect determined by the electron number in each layer [see the inset of Fig. 2 (c)]. As shown in Fig. 2 (c) with system sizes up to 20 electrons, the finite size scaling indicates gapped pseudospin excitation for the case with even electron number in each layer, while it is gapless when the electron number in each layer is odd. The finite pseudo-spin excitation gap is consistent with the disappearance of linear dispersion showed in energy dispersion curve.

Fig. 2 (d) shows the energy gap $\Delta_E(d) \equiv E_1(d) - E_0(0)$ between two lowest energy states for different electron number systems, one can find that the cusp due to the level crossing for the lowest energy excitations near the transition point $d_{c1} \approx 1.1$ is very robust and does not depend on the lattice size, indicating the intrinsic property of such a transition. Clearly, we have identified a transition from the gapless pseudospin FMLRO state at smaller distance to the intermediate phase with new low-lying excitation and a finite pseudospin gap.

Berry Curvature and Energy Spectrum Under Twisted Boundary Conditions.— The transition near $d_{c1} \approx 1.1$ can also be identified by the pseudospin Berry curvature $F(\theta_x^\alpha, \theta_y^\beta)$ and the energy spectrum under twisted boundary conditions. Physically, a gap state has a well-defined smooth Berry curvature, while a gapless state may have singular Berry curvature associated with gapless points in low energy spectrum. Fig. 3 (a) and (b) show the Berry cur-

vatures at the $d < d_{c1}$ and $d_{c1} < d < d_{c2}$ by applying $\theta_x^1 = \theta_x$, $\theta_x^2 = 0$ and $\theta_y^1 = 0$, $\theta_y^2 = \theta_y$ for the lowest energy state in the sector (π, π) . Fig. 3 (a) shows the strong fluctuation of the Berry curvature in FMLRO phase, suggesting the gapless pseudospin spectrum when $d < d_{c1}$. The Berry phase is not well defined due to near level crossing (with Berry phase integrated over each singular point only defined up to the fractional part of 2π), which gives rise to the non-quantized drag Hall conductance in this regime³⁷. Since the Hall conductance in the symmetric channel is well defined in this regime, the non-quantized drag Hall conductance indicates gapless feature of the antisymmetric channel. On the other hand, the Berry curvature is near flat without any singularity in $d_{c1} < d < d_{c2}$ regime [see Fig. 3 (b)], which is consistent with the well-defined single pseudospin excitation gap in this phase. We also find the integral of the Berry curvature gives us zero drag Hall conductance in the intermediate phase. We find that Berry curvatures in all four sectors $(0, 0)$, $(0, \pi)$, $(\pi, 0)$, (π, π) always have similar features and twisting boundary phases will connect the ground state (π, π) to the other three states. In Fig. 3 (c) and (d), one can find the energy spectrum of the lowest two states in the same momentum sector $(K_x, K_y) = (\pi, \pi)$ with twisted phases. Here, we map the phase θ_x, θ_y into one-dimensional quantity $\theta \equiv 10\theta_x + \theta_y$ for convenience of plotting. The singularity in the Berry curvature for $d < d_{c1}$ origins from the energy level crossing as the bilayer relative boundary phase θ_y approaching 2π in contrast to the behavior in the $d > d_{c1}$ regime, where a small gap opens to separate the lowest two states. Based on the above analysis, we confirm that the pseudospin Berry curvature also indicates the phase transition taking place near d_{c1} .

Exciton Superfluid Stiffness.—The FMLRO exciton condensation state is a superfluid for smaller layer separations. To study the evolution of superfluidity with the layer distance, we obtain the exciton superfluid stiffness ρ_s by adding a small twist boundary phase³⁷, which is proportional to the superfluid density and identifies the energy cost when one rotates the order parameter of the magnetically ordered system by a small angle. In our ED calculation, the exciton superfluid stiffness

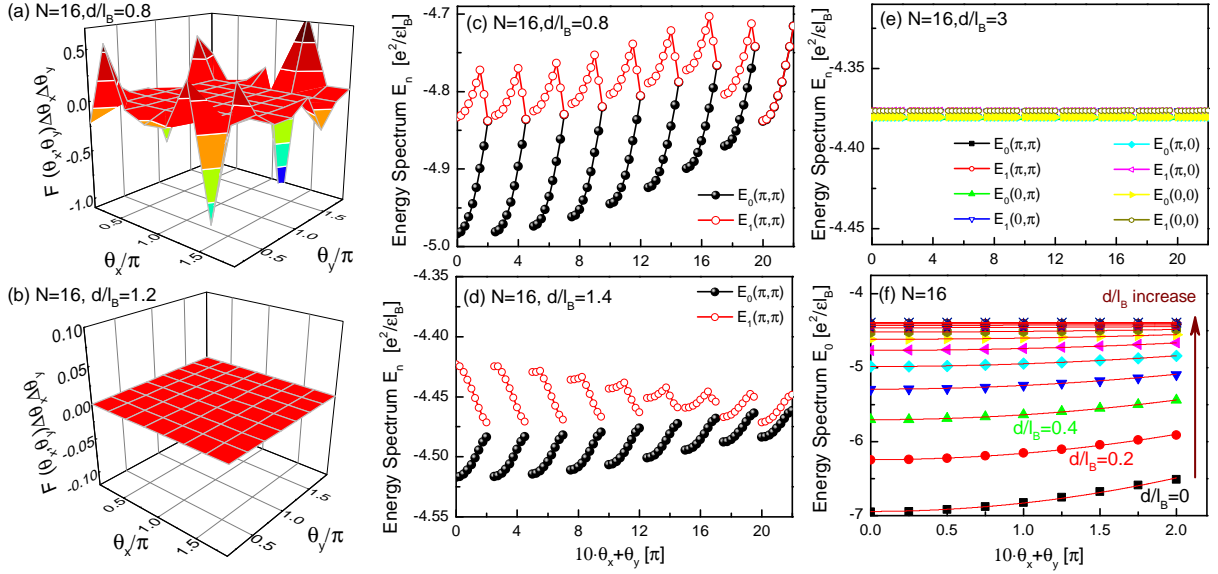


Fig. 3: (Color online) The Berry curvature $F(\theta_x^\alpha, \theta_y^\beta)$ for $d/l_B=0.8$ (a), $d/l_B=1.2$ (b). Here, $\Delta\theta_x$ and $\Delta\theta_y$ are the interval of mesh in phase space. It has strong fluctuation in FMLRO phase shown in (a), while it is smooth in the intermediate phase shown in (b). (c) to (e) are energy spectrum of $N = 16$ system with twisted boundary phases for $d/l_B=0.8$ (c), $d/l_B=1.4$ (d) and $d/l_B=3$ (e). By fitting the energy spectrum with twisted phases, one can get the exciton superfluid stiffness ρ_s [see Eq. 3] (f), which decreases with the layer distance and finally vanishes for $d > d_{c2}$. (f) From bottom to top, d/l_B increases from $d/l_B = 0$ with interval 0.2.

can be obtained according to

$$E(\theta_t)/A = E(\theta_t = 0)/A + \frac{1}{2}\rho_s\theta_t^2 + O(\theta_t^4), \quad (3)$$

where $E(\theta_t)$ is the ground-state energy with twisted (opposite) boundary phases θ_t between two layers $\theta_t = \theta_x^1 - \theta_x^2$ ($\theta_y^{1,2} = 0$), $A = |\mathbf{L}_x \times \mathbf{L}_y|$ is the area of the torus surface. Fig. 3 (c) to (e) show the energy spectrum as a function of twisted phases for different layer distance. At smaller layer separation, one can find the ground state energy increases with tuning the twisted phases [see Fig. 3 (c) and (d)]. By fitting the energy curve using the quadratic function [see Fig. 3 (f)], we get the exciton superfluid stiffness ρ_s , which decreases with the increase of the layer distance, and finally falls down to a negligible value for $d > d_{c2}$ [see Fig. 1]. As shown in Fig. 3 (e), the energy almost does not change with the twisted phases for larger distance, indicating the vanish of pseudospin superfluidity and the decoupling of two layers for $d > d_{c2}$, corresponding to CFL states.

Summary.— In this paper, we study the phase diagram of $\nu = 1/2 + 1/2$ bilayer quantum Hall systems on torus by ED. By studying the energy spectrum, pseudospin excitation gap, exciton superfluid stiffness and Berry curvature, we obtain a phase diagram with the FMLRO phase on the small layer distance side, and CFL phase on the larger distance side separated by an intermediate phase. The new intermediate phase we identified here has distinct features from FMLRO and CFL phases. It has a finite pseudospin gap, finite exciton superfluid stiffness and zero drag Hall conductance. Earlier ED study of such systems on sphere shows that the excitonic superfluid

phase (“111 state”) and the CFL phase are possibly connected via an intermediate phase characterized by the p -wave paired composite fermions^{40,41}, which does not agree with the characteristic features for the intermediate phase we demonstrated here. In an earlier ED simulation on torus³⁷ with including random disorder scattering (limited to electron number $N = 12$), a phase diagram with a direct transition from the superfluid phase to the CFL was obtained, which may be consistent with current results as the superfluid density is indeed nonzero up to the critical point d_{c2} where a transition to the CFL takes place. The weak disorder system may have two scenarios, one is that the pseudospin gap may be nonzero for the intermediate $d = 1.1 \sim 1.8$ regime indicating two phases inside the superfluid regime, or the gapped phase may have a transition back to a weak superfluid phase with gapless excitations driven by weak disorder scattering as the pseudospin gap is very small even in the pure limit. We also comment that although we push the system size to 20 electrons by ED, it still cannot rule out the finite size effect in numerical calculation. Based on our ED calculation, the energy evolves smoothly for both the first order and second order derivative curves[see supplementary materials]. Thus the transition between different phases can be higher order continuous transitions, possibly of the Kosterlitz-Thouless type, which we leave for future study.

We acknowledge helpful discussions with I. Sodemann, T. Senthil, L.J. Zou, M. Zaletel, Z. Papić, S. D. Geraedts, H. Isobe, Y.Z.You. Z.Z. and L.F. are supported by the David and Lucile Packard foundation. L.F. is also supported by the DOE Office of Basic Energy Sciences, Division of Materials Sciences and Engineering under Award No. DE-SC0010526. D.N. Sheng is supported by the U.S. Department of Energy,

Office of Basic Energy Sciences under grants No. DE-FG02-06ER46305. D.N. Sheng was also supported in part by the Gordon and Betty Moore Foundation's EPIQS Initiative, grant GBMF4303 during her visit at MIT. Part of the simulation

were preformed by using the Extreme Science and Engineering Discovery Environment (XSEDE), which is supported by National Science Foundation grant number ACI-1053575.

- ¹ S. M. Girvin and A.H. MacDonald, Perspectives in Quantum Hall Effects, edited by A. Pinczuk and S. Das Sarma (Wiley, New York, 1997).
- ² J. P. Eisenstein and A. H. Macdonald, Nature **432**, 691 (2004).
- ³ B. N. Narozhny and A. Levchenko, Rev. Mod. Phys. **88**, 025003 (2016), and the references therein.
- ⁴ J. P. Eisenstein, Annu. Rev. Condens. Matter Phys. **5**, 159 (2014), and the references therein.
- ⁵ Y. W. Suen, L. W. Engel, M. B. Santos, M. Shayegan, and D. C. Tsui, Phys. Rev. Lett. **68**, 1379 (1992);
- ⁶ J. P. Eisenstein, G. S. Boebinger, L. N. Pfeiffer, K. W. West, and S. He, Phys. Rev. Lett. **68**, 1383 (1992).
- ⁷ D.-K. Ki, V. I. Fal'ko, D. A. Abanin, and A. F. Morpurgo, Nano Lett. **14**, 2135 (2014);
- ⁸ A. Kou, B. E. Feldman, A. J. Levin, B. I. Halperin, K. Watanabe, T. Taniguchi, and A. Yacoby, Science **345**, 55 (2014);
- ⁹ P. Maher, L. Wang, Y. Gao, C. Forsythe, T. Taniguchi, K. Watanabe, D. Abanin, Z. Papi, P. Cadden-Zimansky, J. Hone, P. Kim, and C. R. Dean, Science **345**, 61 (2014).
- ¹⁰ X.-G. Wen and A. Zee, Phys. Rev. Lett. **69**, 1811 (1992).
- ¹¹ K. Moon, H. Mori, Kun Yang, S. M. Girvin, A. H. MacDonald, L. Zheng, D. Yoshioka, and Shou-Cheng Zhang, Phys. Rev. B **51**, 5138 (1995).
- ¹² Kun Yang, K. Moon, Lotfi Belkhir, H. Mori, S. M. Girvin, A. H. MacDonald, L. Zheng, and D. Yoshioka, Phys. Rev. B **54**, 11644(1996).
- ¹³ L. Balents and L. Radzihovsky, Phys. Rev. Lett. **86**, 1825 (2001).
- ¹⁴ Ady Stern, S. M. Girvin, A. H. MacDonald, and Ning Ma, Phys. Rev. Lett. **86**, 1829 (2001);
- ¹⁵ B. I. Halperin, Helv.Phys.Acta **56**,75 (1983).
- ¹⁶ D. Yoshioka, A. H. MacDonald, and S. M. Girvin,Phys. Rev. B **39**, 1932 (1989).
- ¹⁷ B. I. Halperin, P. A. Lee, and N. Read, Phys. Rev. B **47**, 7312 (1993).
- ¹⁸ V. Kalmeyer and S.-C. Zhang, Phys. Rev. B **46**, 9889 (1992).
- ¹⁹ E. Rezayi and N. Read, Phys. Rev. Lett. **72**, 900 (1994).
- ²⁰ J. K. Jain, Composite Fermions (Cambridge University Press, Cambridge, England, 2007); J. K. Jain, Phys. Rev. Lett. **63**, 199 (1989); J. K. Jain, Annu. Rev. Condens. Matter Phys. **6**, 39 (2015).
- ²¹ D.T. Son, Phys. Rev. X **5**, 031027 (2015).
- ²² R. Cote, L. Brey, and A. H. MacDonald, Phys. Rev. B **46**,1010250 (1992).
- ²³ N. E. Bonesteel, I. A. McDonald, and C. Nayak, Phys. Rev. Lett. **77**, 3009 (1996).
- ²⁴ Y. B. Kim, C. Nayak, E. Demler, N. Read, and S. Das Sarma, Phys. Rev. B **63**, 205315 (2001).
- ²⁵ Y.N.Joglekar and A.H.MacDonald, Phys. Rev. B **64**, 155315 (2001).
- ²⁶ A. Stern and B. I. Halperin, Phys. Rev. Lett. **88**, 106801 (2002).
- ²⁷ M. Veillette, L. Balents, and M.P.A. Fisher, Phys. Rev. B **66**, 155401 (2002).
- ²⁸ S. H. Simon, E. H. Rezayi, and M. V. Milovanovic, Phys. Rev. Lett. **91**, 046803 (2003).
- ²⁹ Daw-Wei Wang, Eugene Demler, and S. Das Sarma, Phys. Rev. B **68**, 165303 (2003).
- ³⁰ J. Alicea, O. I. Motrunich, G. Refael, and Matthew P. A. Fisher, Phys. Rev. Lett. **103**, 256403 (2009).
- ³¹ R. Cipri and N. E. Bonesteel,Phys. Rev. B **89**, 085109(2014).
- ³² Hiroki Isobe, Liang Fu, arXiv:1609.09063.
- ³³ Inti Sodemann, Itamar Kimchi, Chong Wang, T. Senthil, Phys. Rev. B **95**, 085135 (2017).
- ³⁴ A. C. Potter, C. Wang, M. A. Metlitski, and A. Vishwanath, arXiv:1609.08618 (2016).
- ³⁵ J. Schliemann, S. M. Girvin, and A. H. MacDonald, Phys. Rev. Lett. **86**, 1849 (2001).
- ³⁶ N. Shibata and D. Yoshioka, J. Phys. Soc. Jpn. **75**, 043712 (2006).
- ³⁷ D. Sheng, L. Balents, and Z. Wang, Phys. Rev. Lett. **91**, 4 (2003).
- ³⁸ S. He, S. Das Sarma, and X. C. Xie, Phys. Rev. B **47**, 4394 (1993).
- ³⁹ K. Park, Phys. Rev. B **69**, 045319 (2004).
- ⁴⁰ G. Möller, S. H. Simon, and E. H. Rezayi, Phys. Rev. Lett. **101**, 176803 (2008).
- ⁴¹ G. Möller, S. H. Simon, and E. H. Rezayi, Phys. Rev. B **79**, 125106 (2009).
- ⁴² M. V. Milovanovic, E. Dobardzic, and Z. Papić, Phys. Rev. B **92**, 195311 (2015).
- ⁴³ R. D. Wiersma, J. G. S. Lok, S. Kraus, W. Dietsche, K. von Klitzing, D. Schuh, M. Bichler, H.-P. Tranitz, and W. Wegscheider, Phys. Rev. Lett. **93**, 266805 (2004).
- ⁴⁴ S.Q. Murphy et al., Phys. Rev. Lett. **72**, 728 (1994).
- ⁴⁵ P. Giudici, K. Muraki, N. Kumada, and T. Fujisawa, Phys. Rev. Lett. **104**, 056802 (2010); P. Giudici, K. Muraki, N. Kumada, Y. Hirayama, and T. Fujisawa, Phys. Rev. Lett. **100**, 106803 (2008).
- ⁴⁶ M. Kellogg, J. P. Eisenstein, L. N. Pfeiffer, and K.W.West, Phys. Rev. Lett. **93**, 036801 (2004); Phys. Rev. Lett. **90**, 246801 (2003).
- ⁴⁷ I. B. Spielman, J. P. Eisenstein, L. N. Pfeiffer, and K. W. West, Phys. Rev. Lett. **84**, 5808 (2000).
- ⁴⁸ E. Tutuc, M. Shayegan, and D. A. Huse, Phys. Rev. Lett. **93**, 036802 (2004).
- ⁴⁹ S. Luin, V. Pellegrini, A. Pinczuk, B. S. Dennis, L. N. Pfeiffer, and K. W. West, Phys. Rev. Lett. **94**, 146804 (2005).
- ⁵⁰ A. D. K. Finck, J. P. Eisenstein, L. N. Pfeiffer, and K. W. West, Phys. Rev. Lett. **104**, 016801 (2010).
- ⁵¹ F. D. M. Haldane, Phys. Rev. Lett. **55**, 2095 (1985).
- ⁵² E. H. Rezayi and F. D. M. Haldane, Phys. Rev. Lett. **84**, 4685 (2000).
- ⁵³ X.G. Wen and A. Zee, Phys. Rev. B **44**, 274 (1991).
- ⁵⁴ Kun Yang and A. H. MacDonald, Phys. Rev. B **63**, 073301 (2001).
- ⁵⁵ D. N. Sheng, Z.-C. Gu, K. Sun, and L. Sheng, Nat. Commun. **2**, 389 (2011).
- ⁵⁶ A. H. MacDonald, P. M. Platzman, and G. S. Boebinger, Phys. Rev. Lett. **65**, 775 (1990).

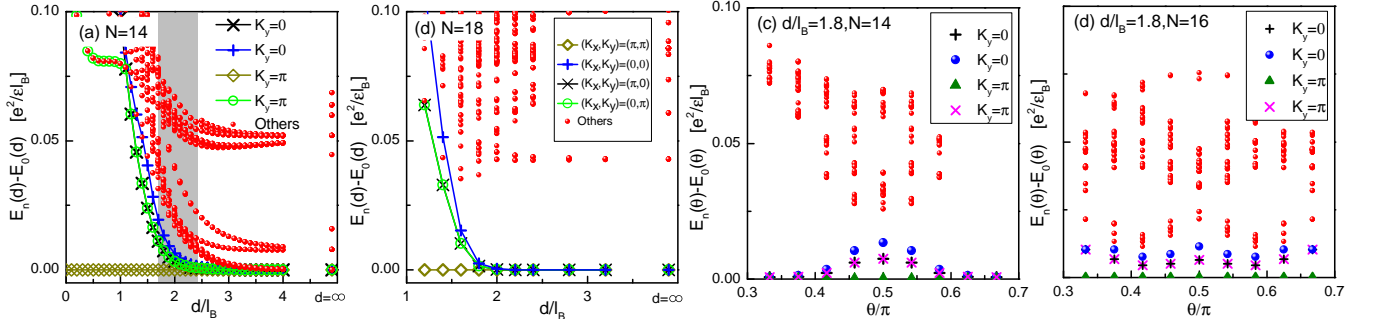


Fig. S1: (Color online) The energy spectrum as a function of layer distance d/l_B for (a) $N = 14$ and (b) $N = 18$ systems. For comparison, the $N = \infty$ data are shown on the rightmost side of each figure. The light grey area indicates the region with a small gap between the lowest four states and higher energy states. For $d/l_B = 1.8$, (c) and (d) show the energy spectrum as a function of the aspect angle θ of the unit cell on torus for $N = 14$ (c) and $N = 16$ (d) systems with layer distance $d/l_B = 1.8$.

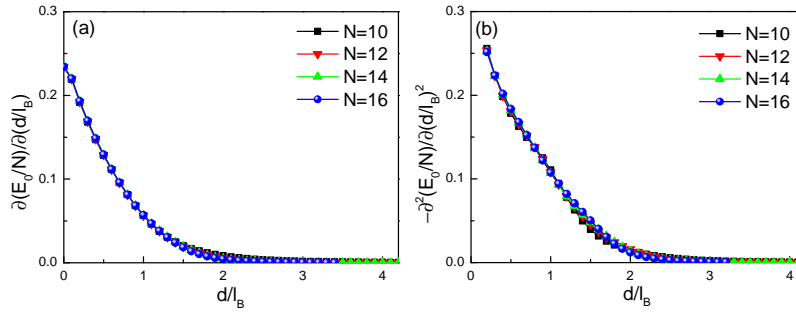


Fig. S2: (Color online) The first-order (a) and second-order (b) derivative curves of ground-state energy E_0/N as a function of layer distance d/l_B . The smooth curves indicate the quantum phase transitions identified in this work may be higher order continuous transitions.

In this supplementary material, we address the finite size effect. From the low energy spectrum shown in Fig. S1 (a), we find indications of the possible four-fold degenerate states in the regime $d/l_B \approx 1.8 \sim 2.4$. We also calculate the energy spectrum at infinite distance [see the rightmost data points in Fig. S1 (a)] to see the evolution of the energy spectrum to the decoupled limit. The four fold degeneracy is generally present for two decoupled CFLs due to the center of mass degeneracy of the electrons separating with other excited states by a gap for finite-size systems. We further calculate the spectrum for $N = 18$ system [see Fig. S1 (b)], which has 9 electrons in each layer forming a completely filled shell in the 3×3 momentum space besides the center of mass double degeneracy in each layer, leading to an extra large gap between the lowest four states and excited states. This indicates the finite size effect and the four-fold degenerate states at finite $d > d_{c2}$ are smoothly connected to the states at the decoupled limit.

The other method to check the robustness of the degeneracy and the finite excitation gap is to change the shape of the unit cell. We obtain the low energy spectrum by varying the aspect angle of the unit cell on torus from $\theta = \pi/3$ to $2\pi/3$, as shown in Fig. S1 (c) and (d) for $N = 14$ and $N = 16$ systems, respectively. The fourfold degeneracy does not change with tuning the geometry of unit cell from hexagon to square for $N = 14$ while it disappears for $N = 16$ system. The $N = 14$ with hexagon unit cell is similar to $N = 18$ system with square unit cell with complete shell filling in momentum space. Based on these analysis, we conjecture that the four-fold degeneracy is due to strong finite-size effect, and the vanishing superfluidity and drag Hall conductance indicate that the quantum state on the $d > d_{c2}$ side is already in the CFL phase.

The transition between different phases should be an open issue in $\nu = 1/2 + 1/2$ bilayer quantum Hall systems. Based on our ED calculation, the energy derivative curves are smooth for both first order and second order curve, as shown in Fig. S2. Thus the transition between different phases can be higher order continuous transitions, possibly of the Kosterlitz-Thouless type, which we leave for future study.